Digital Landscape Architecture Design Combining 3D Image Reconstruction Technology

Chen Chen
School of Environmental Art and Design, Wuxi Vocational Institute of Arts & Technology, Yixing, Wuxi, China

***Abstract*—To achieve better digital landscape design and visual presentation effects, this study proposes a digital landscape design method based on improved 3D image reconstruction technology. Firstly, a precise point cloud registration algorithm combining normal distribution transformation and Trimmed iterative nearest point algorithm is proposed. A color texture method for 3D models is designed in terms of 3D reconstruction, and a visual scene, 3D reconstruction method based on RGBD data is constructed. Secondly, knowledge networks are introduced to assist in the intelligent generation and planning of plant communities in urban landscape scenes. The knowledge network established through the plant database integrates the principles of landscape design and optimizes the layout of landscape plants in urban parks. The running speed and accuracy of research algorithms were superior to traditional methods, especially in terms of registration performance. Compared to the other two algorithms, the registration time of the research algorithm was reduced by 2%, and the errors were reduced by 71.4% and 87.5%, respectively. The panoramic quality of research methods fluctuated within a small range of 0.8 or above, while traditional methods exhibited instability and lower quality. The landscape design generated by research methods was more aesthetically pleasing and harmonious with the actual landscape in terms of plant selection and layout. The proposed method follows the principles of eco-friendly design and demonstrates significant potential for application in the field of urban landscape design.**

Keywords*—3D image reconstruction; PSO; gardens; RGBD; digital landscape

I. INTRODUCTION

Landscape refers to the landscape environment created artificially within a certain area. Through the layout and combination of plants, land, water, architecture, and other elements, as well as the artistic treatment and transformation of natural and cultural elements, it creates a living, working, or leisure place with beauty, comfort, and functionality [1-2]. China's landscape architecture has a rich historical background, and modern landscape architecture has a development history of over 60 years in China [3]. The traditional garden aesthetics advocate harmonious coexistence with nature, reflecting profound humanistic ideas. Research has shown that exposure to nature and green spaces is beneficial for human psychological and physical health. Landscape design has improved urban air quality and provided leisure spaces beneficial to physical and mental health [4]. However, in the face of today's diverse needs, traditional design methods are unable to meet the requirements of rapid urban development and high standard, scientific urban spatial planning.

Digitization has brought challenges to the development of landscape design, but also new opportunities [5]. In response to the limitations of existing landscape evolution models, scholars such as Steer have proposed an innovative modeling technique. This technology achieved one-dimensional sorting and effective propagation of terrain change information by applying linear flow power equations and utilizing directed acyclic graphs. This modeling method could accurately simulate the dynamic changes of the landscape even under conditions of uneven or varying rise and fall rates [6]. In landscape design, the use of sound elements was limited to noise management. Therefore, Luo Ma L et al. explored the impact of sound as a design element on the immersion of architecture and planning in virtual reality environments. This study constructed a virtual reality scene based on field recording to simulate the sound environment. It emphasized the role of audible sound in enhancing landscape design [7]. Wang et al. proposed a landscape water flow design method based on the principles of open channel hydraulics, which combines hydrology and hydraulics as well as landscape processes of infiltration and evapotranspiration. This method could accurately generate flow profiles between depressions in the landscape [8]. The above research indicates that digitalization in the field of landscape architecture mainly focuses on technological application, and in-depth research on design methods and logic is still in its early stages and has not been widely applied in practice. The digitization of traditional garden landscapes still faces challenges, including a lack of unified guidance frameworks and government level norms. In addition, the high cost of technological equipment and the lack of interdisciplinary knowledge have constrained the development of professional talents and the growth of digital design demand.

Three dimensional reconstruction (3DR) is the process of restoring the 3D information of objects in a visual scene through 2D image data or 3D point cloud data (3D-PCD). One type of technology is based on 2D image data, using multiple captured image sequences to construct a color 3D model through feature point matching technology. Another type is based on 3D-PCD, which processes data from multiple collection points and reproduces physical objects through noise reduction, integration, and simulation processes [9]. Researchers such as Xu proposed the use of Hermite radial basis function algorithm combined with RGBD camera, and introduced curvature estimation and confidence score methods to address the common problems of cumulative error and reconstruction distortion in the field of 3D model reconstruction. This method effectively reduced the impact of noise and optimized the results of 3DR [10]. Zhang et al. proposed a 3DR method for motion blurred images using deep learning. This algorithm combined

bilateral filtering denoising theory with Wasserstein generated adversarial networks to remove motion blur, and used the deblurred images generated by this algorithm for 3D reconstruction. This algorithm has been proven to have better deblurring effects and higher efficiency than other representative algorithms [11].

Although many techniques and methods have been proposed in the existing landscape design research, there are still some deficiencies. First, the modeling technique of Steer et al., linear flow power equation models, may lack flexibility in the dissemination of terrain change information. The sound element design method studied by Luo Ma et al. is only applied in noise management, and its effect on improving landscape immersion is limited. The flow design method proposed by Wang et al. is difficult to accurately simulate complex landscape flow in practical applications. In addition, most of these researches focus on the technical application, and the in-depth research on the design method and logic is still insufficient, and the application in practice is limited. In this paper, an accurate point cloud registration algorithm combining normal distribution transformation and trimmed iteration nearest point algorithm is proposed. The color texture method of 3D model is designed from the perspective of 3D reconstruction, and a 3D reconstruction method of visual scene based on RGBD data is constructed. Knowledge network is introduced to assist the intelligent generation and planning of plant communities in urban landscape scenes. The knowledge network established by plant database integrates the principles of landscape design and optimizes the layout of landscape plants in urban parks. It only enhances the aesthetics of the plant selection and layout, is more in tune with the actual landscape, and also follows the principles of eco-friendly design. This study aims to overcome the limitations of traditional design methods, optimize landscape design process by using digital technology and 3D image reconstruction technology, and improve design quality and efficiency. Enhance the aesthetics and coordination of the design by introducing intelligent plant community generation and planning.

This study is divided into five sections. Section I outlines the importance of landscape design and its benefits to human health, introduces the application of digital technology in landscape design and the criticality of 3D reconstruction technology. In Section II, a 3D reconstruction technique based on RGBD data (3DIR) and an improved Poisson surface reconstruction algorithm are described in detail. A method to generate 3D color model based on RGB information is proposed, which is optimized globally by the inner heuristic algorithm and the outer particle swarm optimization algorithm. Section III verifies the effectiveness of the algorithm through experiments, and shows its advantages in registration accuracy and running speed. Section IV and Section V emphasize the importance of DLD methods in improving design efficiency and visualization level, and proposes future research directions for combining deep learning algorithms to improve existing algorithms.

II. Methods and Materials

A. 3DR Method for Visual Scenes Based on RGBD Data

3DIR technology plays a crucial role in landscape design. To obtain a complete 3D scene, it is necessary to address the issue of limited viewing angles caused by a single Azure Kinect DK camera [12]. For this purpose, point cloud registration (PCR) technology can be used to integrate multiple scanned point cloud data. For 3DIR in landscape design, voxel grid downsampling is a more suitable choice, as it can effectively reduce data volume while preserving the overall geometric structure of the scene [13]. For the rough position between two frames of point cloud data, this study adopts a method based on point features to describe local features. The sample consistency initial alignment (SAC-IA) algorithm is a coarse registration method based on point cloud feature description. The algorithm steps are as follows: The first is to select some sampling points from point clouds P and Q, and use the feature description algorithm to perform feature analysis on these points, ensuring that the distance between sampling points exceeds the predetermined minimum value. Afterwards, to find the points in Q that match the features of P, forming a matching point pair P_c. Calculating the rotation and translation matrices of P_c through singular value decomposition (SVD), and then calculating the distance error between registered points. The registration performance is evaluated through the Huber loss function, and the calculation process is Eq. (1).

$$\begin{cases} H\left(l_i\right)=\begin{cases}\frac{1}{2}l_i, \|l_i\|<\delta_i \\ \frac{1}{2}\delta_i\left(2\|l_i\|-\delta_i\right), \|l_i\|>\delta_i\end{cases} \\ H_i=\sum_{i=1}^{n} H\|l_i\| \end{cases} \tag{1}$$

In Eq. (1), $H_i=\sum_{i=1}^{n} H\|l_i\|$. δ represents a pre-set value. l_i represents the distance difference after the rotation and translation transformation of the corresponding point in Group i. By repeatedly matching sampling points and iteratively calculating, the rigid body transformation matrix that causes the minimum distance error is found. The optimal matrix represents the preliminary PCR results. Due to the SAC-IA algorithm reducing the point cloud resolution before feature calculation, some feature information is lost, making it more suitable for rough registration. Afterwards, to perform precise registration on the point cloud. Iterative closest point (ICP) algorithm and its improved algorithms are currently the most classic point cloud accurate registration algorithms. The Trimmed ICP algorithm is an improved algorithm based on ICP that uses minimum truncated multiplication to eliminate excessive distances [14]. The step is to first determine the nearest neighbor point q_i in the baseline point cloud Q for each point p_i in point cloud P, and calculate its distance squared d_i^2. These distances are sorted in ascending order, and the first N points are selected to form a subset P_s, then the sum of the squared distances S of this subset is calculated. The number of reserved points is determined based on the number N_p of the point cloud to be registered. The process is given in Eq. (2).

$$N = kN_p \quad (2)$$

Using the SVD method to solve the set of reserved points obtained from the calculation, the point cloud rotation translation matrix is obtained, as shown in Eq. (3).

$$(R,T) = \arg\min \sum_{i=1}^{N} \left\| q_i - (Rp_i + T) \right\| \quad (3)$$

After applying the rotation matrix to transform the registration point cloud P, it is necessary to re estimate the corresponding point relationship with the reference point cloud Q. The iterative process continues until the number of iterations exceeds the preset limit, and the mean square error $\frac{S}{N}$ value of the point pairs drops below the set threshold, or when the similarity between the results of two consecutive iterations is extremely high, the final registration result can be obtained. The normal distribution transform (NDT) algorithm is a high registration accuracy and fast computational speed PCR [15-16]. To achieve better registration results, it is combined with the Trimmed ICP algorithm. The improved PCR steps are shown in Fig. 1.

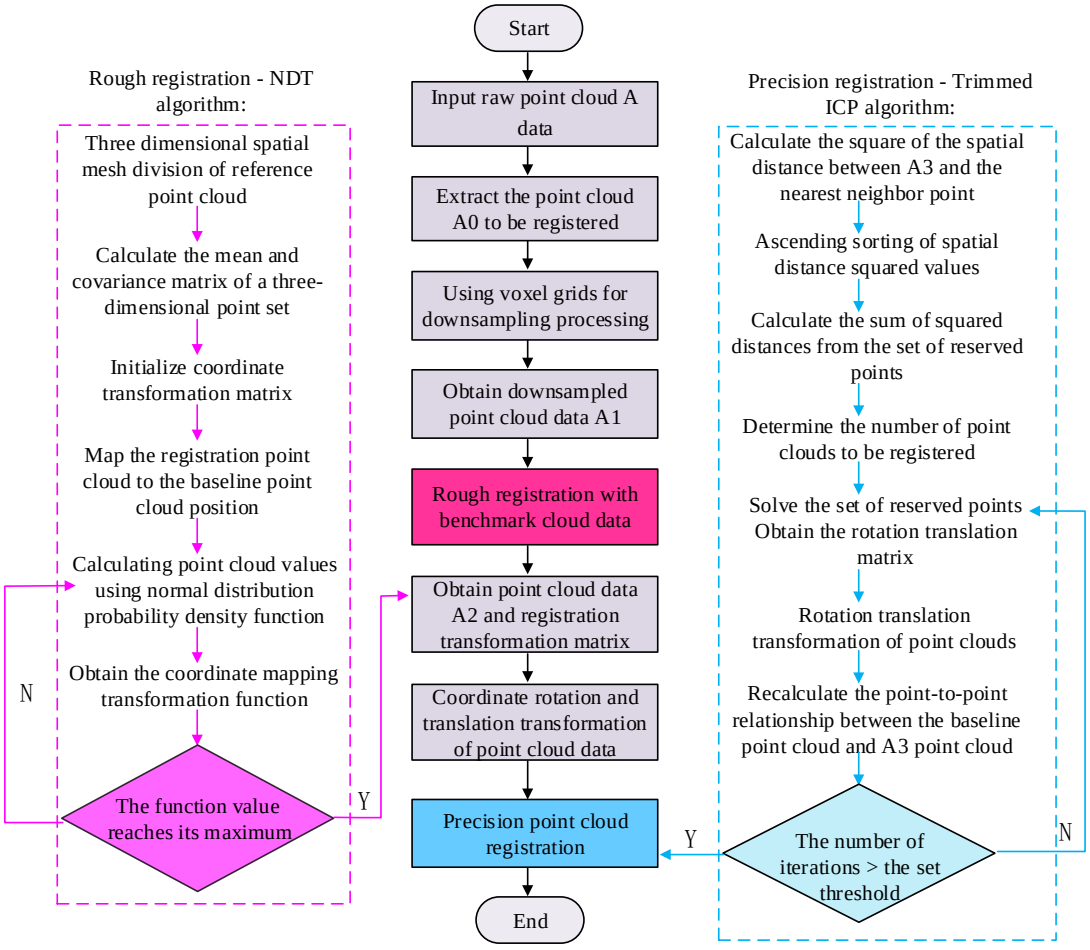

Fig. 1. Point cloud registration process.

In Fig. 1, PCR first speeds up registration by reducing the amount of data in point cloud P, and uses voxel grid downsampling algorithm to obtain simplified point cloud $\hat{P}_0$. Preliminary to use the NDT algorithm to complete rough registration of $\hat{P}_0$ and benchmark point cloud Q, obtaining transformation matrix M_1 and registered point cloud $\hat{P}_1$. Applying M_1 to transform the original point cloud P again to obtain a rough alignment point cloud P_1. Finally, the Trimmed ICP algorithm is used to finely adjust the registration of $\hat{P}_1$ and Q, obtaining the final accurate registration point cloud $\hat{P}_2$ and its corresponding rotation translation matrix M_2. Point cloud 3DR is the process of generating a 3D surface mesh model based on the target point cloud obtained through algorithmic processing. 3D surface reconstruction techniques can be divided into two types: triangulation based mesh and surface fitting. The surface fitting algorithm generates a model close to the solid surface through function solving, which is insensitive to noise. The advantage of Poisson's algorithm lies in its ability to resist noise, producing clear contours and strong closure of the model. The steps for reconstructing Poisson's surface are shown in Fig. 2.

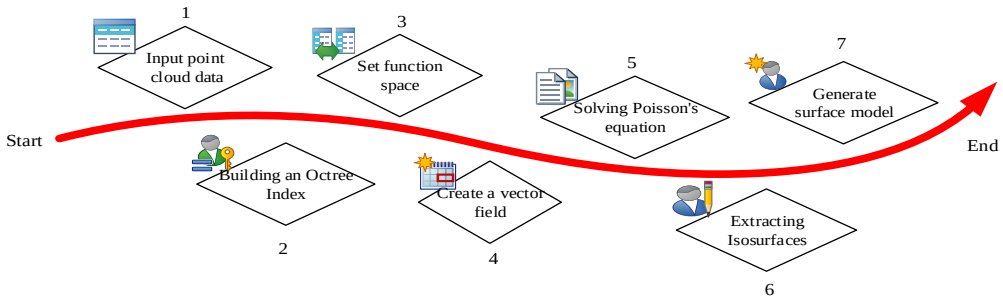

Fig. 2. Poisson surface reconstruction steps.

The original Poisson reconstruction algorithm is susceptible to errors, resulting in hidden function shifts. Someone proposed a masked Poisson surface reconstruction algorithm based on the original Poisson reconstruction algorithm. The improved method introduces a penalty function to limit offset and assigns weight ω to each point in point cloud P. The improved Poisson equation $E(\chi)$ can be represented by Eq. (4).

$$E(\chi)=\int\left\|\vec{V}(q)-\nabla\chi(q)\right\|^2 dp+\frac{\alpha S(P)}{\sum_{q\in P}\omega(q)}\sum_{q\in P}\omega(q)\chi^2(q) \quad (4)$$

In Eq. (4), $\vec{V}(q)$ represents the vector field. $\chi(q)$ represents the indicator function. $\omega(q)$ represents the weight of the sample, with a value of 1. α represents the equilibrium coefficient. $S(P)$ represents the surface area after reconstruction. To minimize Eq. (4) and define an operator to represent it as a masked Poisson equation. The calculation process is Eq. (5).

$$(\Delta-\alpha_s\oplus)\chi=\nabla\cdot\vec{V} \quad (5)$$

To solve the Poisson equation, the algorithm uses discretization methods to construct a linear equation system $Ax=b$ and apply zero constraint conditions at the sample points, and solves the coefficients to obtain matrix A. The cascaded multigrid method is used to optimize the solution process, adjusting weights at different depths d to maintain surface morphology and refine estimation. The scale invariance of the reconstruction effect is achieved by scaling the point set, adjusting functions $E_V\left(\tilde{\chi}\right)$ and $E_{\tilde{\omega},\tilde{p}}\left(\tilde{\chi}\right)$, and redefining weight values $\tilde{\omega}(p)$. The new set of points can be represented as $\left(\tilde{\omega},\tilde{P}\right)$, and the function is Eq. (6).

$$\begin{cases} E_V\left(\tilde{\chi}\right)=\int\left\|\vec{V}(q)-\nabla\chi(q)\right\|^2 dp=\frac{1}{2}E_{\tilde{V}}(\chi) \\ E_{\tilde{\omega},\tilde{p}}\left(\tilde{\chi}\right)=\frac{\alpha_s S(P)}{\sum_{q\in P}\omega(q)}\sum_{q\in P}\omega(q)=\frac{1}{4}E_{\tilde{\omega},\tilde{p}}(\chi) \end{cases} \quad (6)$$

In addition, the algorithm optimized the handling of boundary conditions, extending Dirichlet boundary conditions to Neumann boundary conditions. This reduces constraints when data is missing, as long as the derivative of the boundary is zero [17]. To enhance the realism of point cloud based 3D models, in addition to shape reconstruction, this study further integrates RGB information to generate 3D color models. In the process of constructing a 3D model of a point cloud, the 3D surface reconstruction algorithm can only establish an object surface model lacking texture details based on the spatial features of the point cloud data. The steps to build this model are as follows: first, to perform normal vector calculation on the original color point cloud data P. The normal vector of a point cloud is generally solved using principal component analysis algorithm, which establishes a covariance matrix C based on the neighboring points within a certain range of 3D point p_0 and solves for its eigenvectors, as shown in Eq. (7).

$$\begin{cases} C=\frac{1}{k}\sum_{i=1}^{k}(p_i-p_0)\bullet(p_i-p_0)^T \\ C\bullet\vec{v}=\lambda\bullet\vec{v} \end{cases} \quad (7)$$

In Eq. (7), k represents the number of nearest neighbors within the neighborhood range of 3D point p_0. The collected color point cloud data containing only XYZRGB information needs to be accompanied by a normal vector to form a dataset with the XYZRGB Normal attribute. By constructing a Kd Tree index for these data, point cloud color mapping can be performed. At this point, for each point on the surface of the model, to use Kd Tree to search for nearby point cloud data points, take the average of their RGB values, and assign the corresponding color texture to the model. In this way, each point can be mapped to generate a 3D surface model with colored textures.

B. DLD of Landscape Architecture Based on 3DIR

The innovation of digital technology has produced new design languages and construction techniques, while bringing innovative structures and forms of expression to traditional landscape design [18]. Knowledge driven and landscape design are closely linked, guiding and promoting the design and implementation of landscape projects through the application of multidisciplinary knowledge and technology. Therefore, this study combines 3DIR technology and uses knowledge networks as the core driver to intelligently generate landscape plant communities in the scene and carry out corresponding planning and layout. Fig. 3 shows the overall framework of DLD.

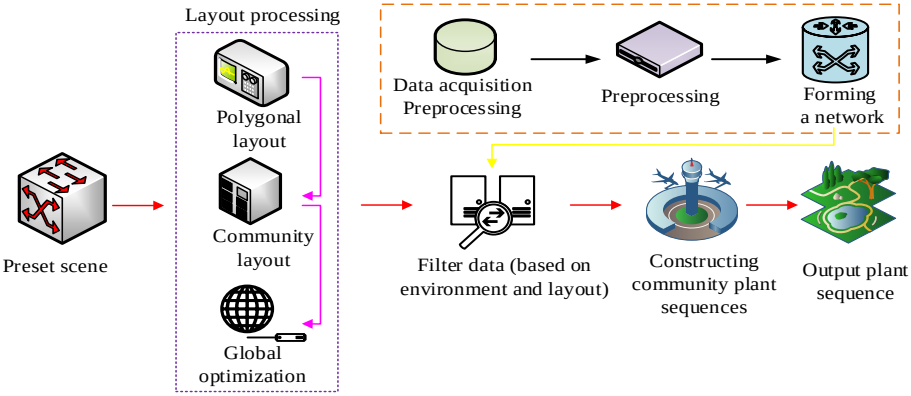

Fig. 3. Digital landscape design model.

The process of DLD in Fig. 3 mainly consists of three steps, which are to build a plant knowledge network, then layout the group within the scene, and finally construct the composition sequence of the community. All three are designed based on data to form a cohesive whole. In terms of data acquisition, most sources come from literature, networks, etc. Data related to landscape plants were collected, which provided fundamental support for this study. Knowledge graphs can provide practical and valuable disciplinary information [19]. Therefore, this study uses knowledge graphs based on undirected graph models to represent landscape plant data. The proposed landscape layout adopts a double-layer optimization strategy: the inner layer uses heuristic algorithms for polygon planning, and the outer layer uses particle swarm optimization (PSO) for global optimization [20]. The inner algorithm is responsible for the preliminary layout design, while the outer algorithm further refines and enhances the design scheme. Among them, heuristic algorithms use simple polygons for layout and find the optimal position within a matrix scene $M=(X,Y)$. Set $P=(P_1,P_2,\ldots,P_m)$ includes polygons, and $\Omega=\{\Omega_1,\Omega_2,\ldots,\Omega_m\}$ contains all possible rotation angles. Scene M has a center point O and marks different areas. Grassland $A=(\sigma_1)$ is a layout area, while buildings, water bodies, and roads $B=(\sigma_2,\sigma_3,\sigma_4)$ are non layout areas. Given a polygon P_i and a translation vector $v=(v_x,v_y)$, to denote $p=(p_x,p_y)$ as the current position of polygon P. The translation function of a polygon is defined in Eq. (8).

$$P_i \oplus v=\left\{\left(p_x+v_x,p_y+v_y\right)\middle|p=\left(p_x,p_y\right)\in P_i,x\in X,y\in Y\right\} \quad (8)$$

If the center of the polygon is represented as P_i, and its state is only determined by its center g_i and rotation angle a_i, then the current polygon calculation formula is Eq. (9).

$$P_i(a_i)=\left\{\begin{pmatrix}g_{ix}+(p_x-g_{ix})\cos(a_i)-(p_x-g_{ix})\sin(a_i),g_{ix}\\+(p_x-g_{ix})\sin(a_i)+(p_x-g_{ix})\cos(a_i)\end{pmatrix}\middle|p\in P_i,a\in\Omega\right\} \quad (9)$$

The unit layout area will be traversed outward from the center of the scene in a circular hierarchical manner, and the current unit layout area is scored using a scoring function $F=\{f_1,f_2,\ldots,f_k\}$, as shown in Eq. (10).

$$\begin{cases}f_1(P_i(a_i))=\left|P_i(a_i)\right|\times\omega_1\\f_2(P_i(a_i))=\left|P_i(a_i)\middle|p\in A\right|\times\omega_2\\f_3(P_i(a_i))=\left|P_i(a_i)\middle|p\in B\right|\times\omega_3\\f_4(P_i(a_i))=\left|P_i(a_i)\middle|p\in(P-P_i)\right|\times\omega_4\\f_5(P_i(a_i))=\left|P_i(a_i)\middle|p\notin(P-P_i),p+d\in(P-P_i)\right|\times\omega_5\end{cases} \quad (10)$$

In Eq. (10), $\omega_1,\omega_2,\ldots,\omega_k\ (-\infty<\omega<+\infty)$ represents the weight of different scoring factors, which depends on the distribution of layout and non layout spaces within the scene. If condition $mscore=\max\{p_{1score},p_{2score},\cdots,p_{nscore}\}$ is met, the polygon is allowed to be positioned in the corresponding region $P_i(a_i)\to M$. Each polygon records its number, type, area, and coordinate information. The layout of plant landscape in landscape design is its core, and the diversity of plant species constitutes its structure. The composition of the community affects the appearance and changes of the landscape, and plants need to be arranged in a polygonal manner, divided into tree, shrub, mixed or blank types. The combination layout of plants is crucial for landscape features, and it is necessary to carefully plan the distribution of plants in the polygon, including the mixed planting forms of different plants. Fig. 4 shows the distribution of some plant communities and their probability of occurrence within the polygon.

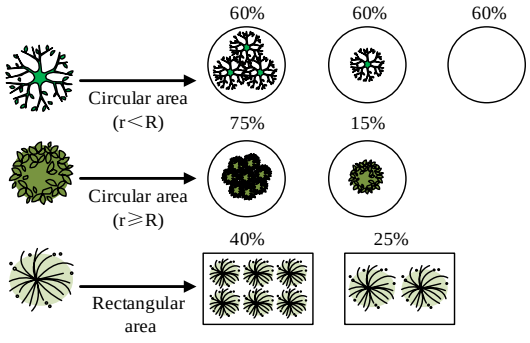

Fig. 4. Distribution of plant communities and their probability of occurrence within the polygon.

In Fig. 4, there are three main requirements for the local layout of the garden landscape. The primary rule is to ensure that the canopy of the trees does not obstruct each other. Secondly, the canopy of shrubs should be independent of each other to ensure that the canopy of shrubs and trees does not intersect. Plants within the same polygon form the same community and inherit polygon parameters from the community. These parameters include the number, type, total area, coordinates, and plant features of the polygons. The plant characteristics provide a detailed description of the number, location, canopy area, building area, and category of trees and shrubs. The polygon layout algorithm effectively arranges plant communities, but if the layout is too neat, it may lack natural beauty. Modern design tends to combine norms with nature to present order and natural beauty. By analyzing the forms of plant space creation, this study proposes the following rules: a single plant is defined as T, the types of trees and shrubs are T_{type}, and the crown coverage area is $C = T_{type}$. The plant community is defined as $G = \{T_1, T_1, \ldots, T_n\}$, and the polygon is defined as $B = \{G_1, G_2, \ldots, G_m\}$. All non-repeating plants are randomly selected and their scores are calculated using Eq. (11).

$$T_{isore} = \sum_{j=1}^{k} q_j(T_i), q \in Q \tag{11}$$

The optimal sequence of plants found based on the scoring function is Eq. (12).

$$\min SEQ(T) = \min \sum_{m}^{1} \sum_{i=1}^{n} \sum_{j=1}^{k} q_j(T_i), q \in Q, T \in G \tag{12}$$

After optimizing the global layout algorithm, plant information, including numbers and parameters, is extracted from the polygon, which serves as the community identifier. These information are included in the plant list, and then suitable plant species are selected in the knowledge network based on specific conditions. Screening involves distribution range, adaptability, and lighting requirements to preliminarily determine candidate species, and then further screen using geographic information and environmental conditions to form plant collection B_s. At the same time, filtering the community database to form a set G_s. The species of plants in set G_s become set B_s. By comparing the set, the final plant candidate set $B_{sg} = B_s \cup B_g$ is formed, and the community set is updated to G_{sg}. The selected community is evaluated based on plant adaptability, cost, and environmental impact, but the community set G_{sg} is not simplified to maintain species diversity. After adjusting the diversity based on the available planting area, a final selection set Q is formed. The community configuration is assigned to plants from set Q, sharing numbers, rather than increasing the average score of selected communities. After the layout is completed, the herbaceous classification within the community is arranged independently and serves as a supplement at the end of the list. This study uses PSO to conduct global optimization on the basis of building a complete plant community. The performance evaluation process of digital design methods for landscape architecture is Eq. (13).

$$S = \lambda_1 \sqrt{\frac{\sum_{1}^{n} \left(q_i(T) - \overline{q_i(T)}\right)^2}{n-1}} + \lambda_2 \sqrt{\frac{\sum_{1}^{n} \left(f_i(P(a)) - \overline{f_i(P(a))}\right)^2}{n-1}} \tag{13}$$

In Eq. (13), both λ_1 and λ_2 will set corresponding values. The design and implementation of the prototype system are completed by packaging the proposed model, standardizing its input and output, and generating AutoCAD exchange files and executable files for the prototype system. The overall architecture of the model is Fig. 5.

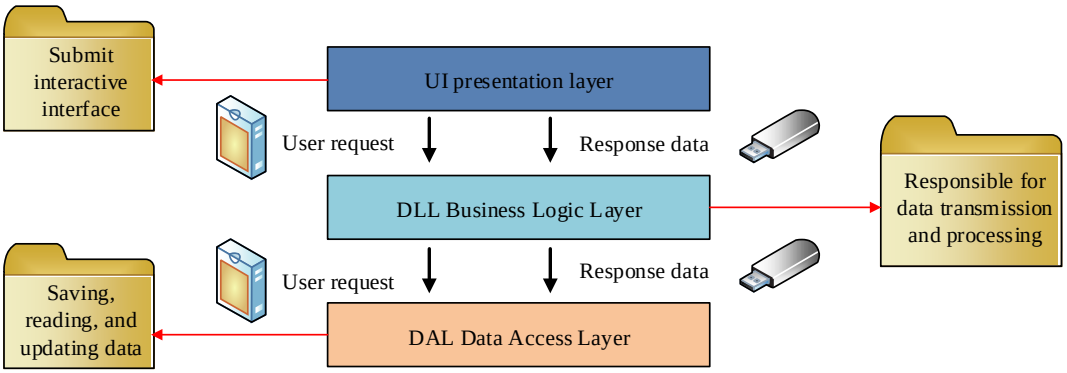

Fig. 5. Digital landscape architecture design model.

In Fig. 5, the presentation layer handles the user interface and interaction, including displaying data and receiving input. The business logic layer is responsible for verifying input parameters, ensuring the stable operation of the program, and performing operations such as data queries and updates. This includes checking for empty text, file path issues, and input legality. The data access layer is responsible for communicating with the database, performing data addition, deletion, modification, and querying operations, and the data objects should only be referenced in this layer to avoid direct data manipulation by other layers.

III. Results

A. 3DR Experimental Analysis of Visual Scenes Based on RGBD Data

To verify the effectiveness of the proposed algorithm, experiments are conducted to compare combination of SAC-IA

or NDT coarse registration and ICP fine registration algorithms based on FPFH, 3DSC, SHOT features. Experiment is performed on i5-9300H CPU Windows 10 system using the environment of Visual Studio 2019 and PCL 1.11.0 library. The Stanford University's Bunny point cloud (BPC) and visual scene point cloud (VSPC) are collected as the dataset. Table I shows the experimental parameters.

PCR experiments are conducted based on the point cloud parameter settings in Table I, and the experimental results are shown in Fig. 6.

TABLE I. EXPERIMENTAL PARAMETER SETTINGS

Experimental project	Parameter	Experimental project（NDT）	Parameter
Leaf nodes (BPC data)	**0.01**	**Minimum Conversion Difference (BPC Data)**	**0.0001**
Leaf nodes (VSPC data)	**100**	**Minimum Conversion Difference (VSPC Data)**	**1**
Search radius (BPC data)	**0.05**	**Parameter Step Size (BPC Data)**	**0.25**
Search radius (VSPC data)	**500**	**Parameter Step Size (VSPC Data)**	**500**
Search radius (feature description algorithm)	**0.5、1000**	**Resolution parameter value**	**0.5、900**
Point cloud overlap parameter value (Trimmed ICP)	**95%**	**Maximum number of iterations (NDT, ICP)**	**50、20**

(a) Initial position (b) FPFH+ICP (c) SHOT+ICP (d) NDT+ICP (e) This article studies

Fig. 6. Registration results of various algorithms.

In Fig. 6, the proposed PCR algorithm and several comparison algorithms can effectively cover the blue point cloud to be registered onto the reference purple point cloud. The SAC-IA algorithm and NDT algorithm have similar registration effects, but compared to the fusion of ICP and NDT registration, the research algorithm is more accurate and shows stronger robustness. The registration running time of each algorithm and the RMSE values of the registered point cloud in various directions are shown in Fig. 7.

In Fig. 7, the research algorithm outperforms other algorithms in terms of running speed and registration accuracy. In algorithms based on local features, the registration of FPFH feature descriptions leads in efficiency and accuracy, while the 3DSC algorithm takes the longest time, several times that of other methods. The NDT algorithm based on statistical probability reduces the running time by at least 69% compared to local feature methods. Fig. 8 shows the comparison results of quantitative indicators based on self-collected point cloud (SCPC) data.

In Fig. 8, in the testing of the Bunny dataset, the root mean square error of the NDT algorithm is lower than that of the algorithm based on local features. On SCPC data, NDT performs poorly, possibly due to a decrease in accuracy caused by the distribution of the data in 3D space. The research algorithm performs better than the NDT algorithm combined with ICP on both types of data, reducing registration time and improving accuracy. Compared with the fusion of ICP and NDT, the registration time of the research algorithm was reduced by 2%, and the RMSE was reduced by 71.4% and 87.5%, respectively, demonstrating good robustness and high registration accuracy. Fig. 9 shows the evaluation index results of each algorithm.

In Fig. 9, compared with the surface fitting based method, the 3D surface reconstruction technique based on mesh triangulation performs poorly. The greedy projection triangulation (GPT) algorithm is lower in key performance indicators than Poisson reconstruction and masked Poisson reconstruction algorithms, with differences of up to 0.010203, 0.000701, and 0.001874, respectively. GPT outperforms the rolling ball algorithm in RMS metrics, reducing by 38.1% and demonstrating better repair performance. In addition, the shielded Poisson algorithm exhibits higher model quality compared to traditional Poisson algorithms.

B. DLD Experimental Analysis

The experiment utilized Rhino software and visual scene 3DR based on RGBD data to construct parameter logic and establish a parameterized analysis model. It selected real garden image data and applied the technology studied to distinguish natural and artificial landscape elements, such as plants and architecture, for instance design. The evaluation indicators for landscape design include panoramic quality, design aesthetics, ease of technical implementation, cultural significance, and urban characteristics. Fig. 10 shows the evaluation of the DLD effect of 3DIR technology.

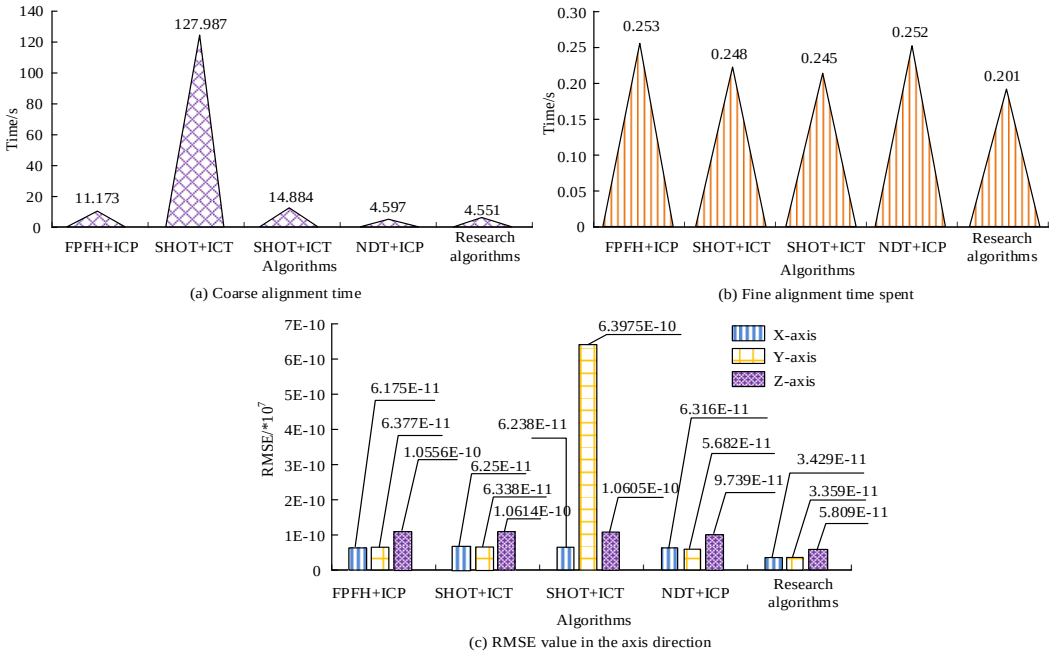

(a) Coarse alignment time (b) Fine alignment time spent

(c) RMSE value in the axis direction

Fig. 7. Comparison of quantitative indicators based on bunny point cloud data.

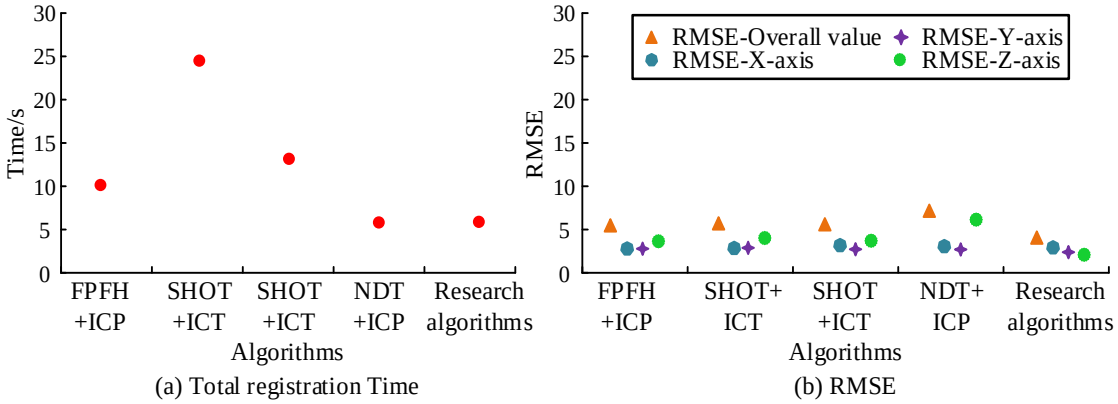

(a) Total registration Time (b) RMSE

Fig. 8. Comparison of quantitative indicators based on scpc data.

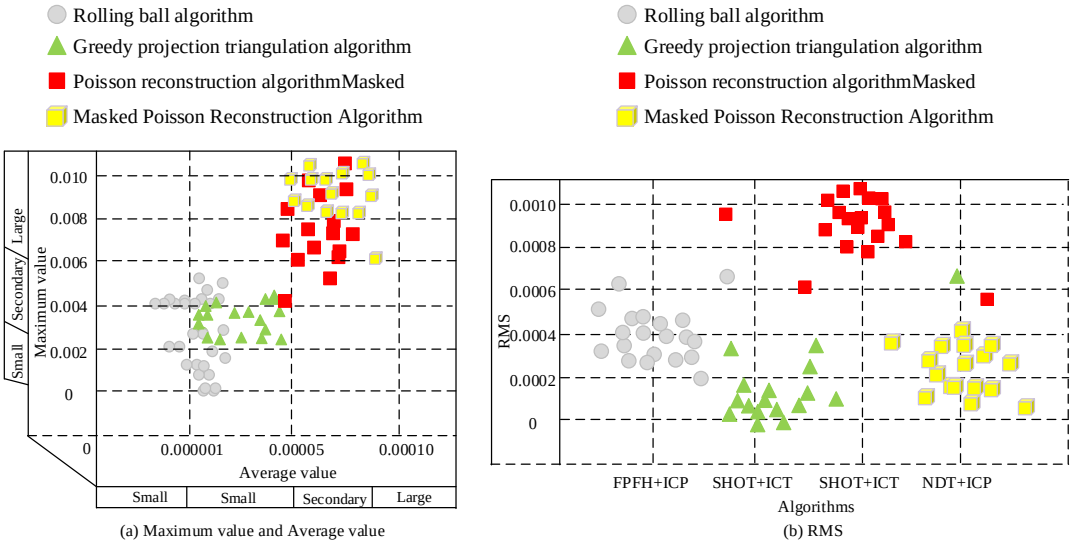

(a) Maximum value and Average value (b) RMS

Fig. 9. Evaluation index results of each algorithm.

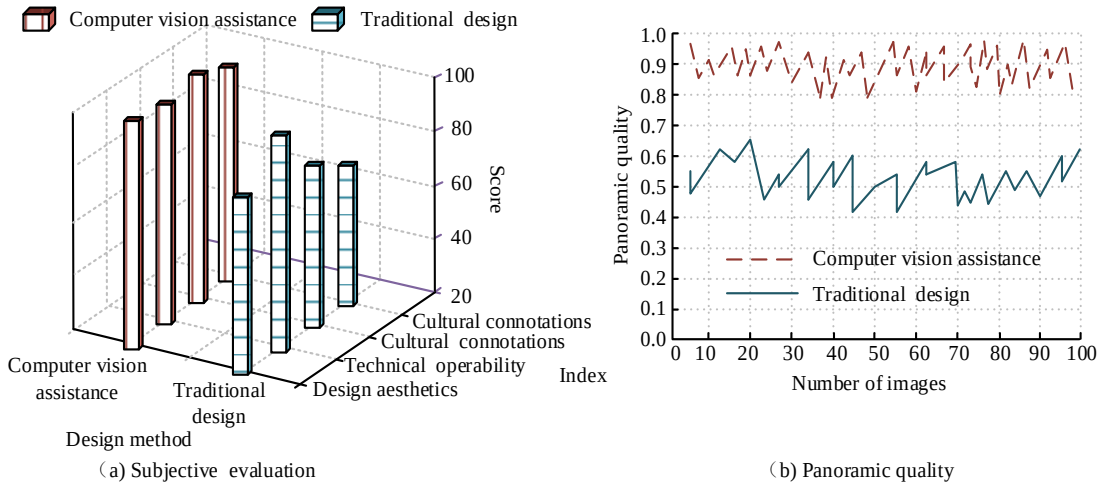

Fig. 10. The design effect of DLD based on 3DIR.

In Fig. 10 (a), the DLD combined with 3DIR technology performs well on a series of subjective evaluation indicators, with all indicators superior to traditional landscape design methods except for technical operability indicators. In Fig. 10 (b), among 100 design samples, the panoramic quality of the research method fluctuates within a small range of 0.8 or above. The stability of panoramic quality in traditional methods is poor, ranging from 0.4 to 0.7. Moreover, the panoramic quality value is relatively low, and the design quality fluctuates continuously with the level of manual design. Fig. 11 shows the performance comparison between the research method and other algorithms.

In Fig. 11, the AUC value of the study method is very close to 0.9, which means that its performance is excellent. Although CNN-GAN performed well in the early stage, the overall curve is not as steep as the study method, and the AUC value should be slightly lower than the study method. It can be inferred from the curve shape that the AUC value of PSO is significantly lower than that of the research method and CNN-GAN, which means that its classification effect is poor. Compared with the other two methods, the performance of the research method is very stable in the whole range. Fig. 12 shows the display of DLD results.

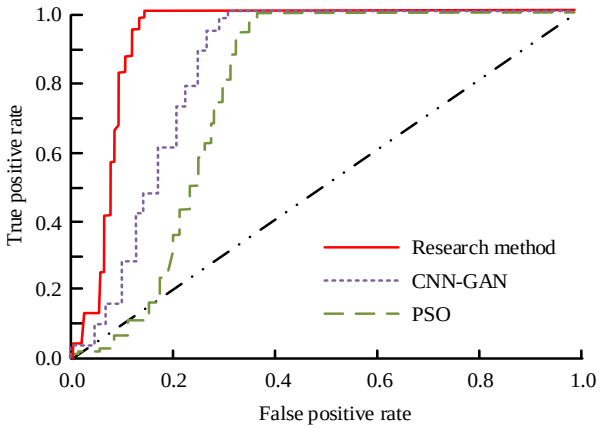

Fig. 11. Convergence process of objective functions of the three algorithms.

Fig. 12 shows the effectiveness of the classic iterative optimization intelligent landscape design algorithm, which generates scenes that are highly consistent with real landscape design, especially in vegetation selection and layout. The research algorithm not only follows the principles of eco-friendly design, but also enhances the aesthetics of plants in the context of urban landscaping, achieving a visual effect of harmonious coexistence between humans and nature.

Fig. 12. Display of DLD achievements.

IV. Discussion

Compared with the modeling technique of Steer et al. [6], the research method is more accurate in dealing with landscape design details, and high-precision 3D reconstruction is achieved through improved point cloud registration and Poisson reconstruction techniques. Studies have shown that this method is superior to Luo Ma L et al. [7] in reconstruction details and to Wang et al. [8] in landscape flow design in overall design performance. Compared with the traditional ICP and NDT methods, the registration time of the proposed algorithm is reduced by 2%, and the error is reduced by 71.4% and 87.5%, respectively. In Bunny point cloud and SCPC data testing, the root mean square error (RMSE) is lower than that of traditional methods, and the run time is significantly reduced. The digital landscape design method based on 3DIR technology has excellent performance in the subjective evaluation indicators such as panoramic quality, design beauty, technical realization difficulty, cultural significance and urban characteristics, and its stability is higher than that of traditional design methods. The resulting landscape design is more aesthetically pleasing and coordinated in plant selection and layout, and intelligent and ecologically friendly plant community layout is assisted by

knowledge networks. The dual optimization strategy, which combines heuristic algorithm and particle swarm optimization, takes into account the beauty and functionality of landscape design. In conclusion, this method has significant advantages and application potential in 3D reconstruction and landscape design.

V. CONCLUSION

To improve the efficiency and visualization level of landscape design, and to help designers quickly and accurately convert elements such as terrain, vegetation, and water in the real world into digital models, this study adopted the concept of DLD to analyze landscape architecture and digital design. Based on the current difficulties in landscape planning and design, a DLD method based on 3DIR technology was proposed. The results show that the proposed algorithm is superior to other algorithms in terms of running speed and registration accuracy. Statistical probability-based NDT algorithms have at least 69% shorter run times than local feature algorithms and lower RMSE on rabbit datasets. Compared with the method combining ICP and NDT, the registration time was reduced by 2% and RMSE was reduced by 71.4% and 87.5%, respectively. The shielded Poisson algorithm is superior to the traditional Poisson algorithm in terms of model quality. The panoramic quality of the research method is stable at 0.8 or above, while the panoramic quality of the traditional design method fluctuates between 0.4 and 0.7 and is low. The scene generated by the research method is highly consistent with the actual landscape design, especially in vegetation selection and layout. In the future, deep learning algorithms will be integrated to improve and innovate traditional algorithms while ensuring PCR rate and registration accuracy.

REFERENCES

[1] Deng Y, Xie L, Xing C, Cai L. Digital city landscape planning and design based on spatial information technology. Neural Computing and Applications, 2022, 34(12): 9429-9440.

[2] Usman A M, Abdullah M K. An Assessment of Building Energy Consumption Characteristics Using Analytical Energy and Carbon Footprint Assessment Model. Green and Low-Carbon Economy, 2023, 1(1): 28-40.

[3] Li D, Li H, Li W, Guo J, Li E. Application of flipped classroom based on the Rain Classroom in the teaching of computer-aided landscape design. Computer Applications in Engineering Education, 2020, 28(2):357-366.

[4] Cui Xing, Du Chunlan. Research on Landscape Parametric Design Based on GIS+BIM Information Model—Taking the Planning and Design Experiment of Mountain Scenic Environment Road as an Example. Chinese Landscape Architecture, 2023, 39(6):39-45.

[5] Li P. Intelligent landscape design and land planning based on neural network and wireless sensor network. Journal of Intelligent and Fuzzy Systems, 2021, 40(2):2055-2067.

[6] Steer P. Short communication: Analytical models for 2D landscape evolution. Earth Surface Dynamics, 2021, 9(5):1239-1250.

[7] Luoma L, Fricker P, Schlecht S. Design with Sound: The Relevance of Sound in VR as an Immersive Design Tool for Landscape Architecture. Journal of Digital Landscape Architecture, 2023, 2023(8): 494-501.

[8] Wang Z, Trauth K M. Development of GIS-based python scripts to calculate a water surface profile on a landscape for wetlands decision-making. Journal of hydroinformatics, 2020,22(3):628-640.

[9] Zhao Y, Luo X, Qin K, Liu G, Chen D, Augusto R S, Liu Z. A cosmic ray muons tomography system with triangular bar plastic scintillator detectors and improved 3D image reconstruction algorithm: A simulation study. Nuclear Engineering and Technology, 2023, 55(2): 681-689.

[10] Xu Y, Nan L, Zhou L, Wang J, Wang C C. Hrbf-fusion: Accurate 3d reconstruction from rgb-d data using on-the-fly implicits. ACM Transactions on Graphics (TOG), 2022, 41(3): 1-19.

[11] Zhang J, Yu K, Wen Z, Qi X, Paul A K. 3D reconstruction for motion blurred images using deep learning-based intelligent systems. Computers, Materials & Continua, 2021, 66(2): 2087-2104.

[12] Liu X, Li J, Lu G. Improving RGB-D-based 3D reconstruction by combining voxels and points. The Visual Computer, 2023, 39(11): 5309-5325.

[13] Li J, Gao W, Wu Y, Liu Y, Shen Y. High-quality indoor scene 3D reconstruction with RGB-D cameras: A brief review. Computational Visual Media, 2022, 8(3): 369-393.

[14] Chen H B, Zheng R, Qian L Y, Liu F Y, Song S, Zeng H Y. Improvement of 3-D ultrasound spine imaging technique using fast reconstruction algorithm. IEEE Transactions on Ultrasonics, Ferroelectrics, and Frequency Control, 2021, 68(10): 3104-3113.

[15] Kermarrec G, Morgenstern P. Multilevel T-spline Approximation for Scattered Observations with Application to Land Remote Sensing. Computer-Aided Design, 2022,146(1):103193-103206.

[16] Thompson P, Dugmore A J, Newton A J, Cutler N A, Streeter R T. Variations in tephra stratigraphy created by small-scale surface features in sub-polar landscapes. Boreas, 2022, 51(2):317-331.

[17] Faust E, Schlüter A, Müller H, Steinmetz F, Müller R. Dirichlet and Neumann boundary conditions in a lattice Boltzmann method for elastodynamics. Computational Mechanics, 2024, 73(2): 317-339.

[18] Mukherjee T, Pucci P, Sharma L. Nonlocal critical exponent singular problems under mixed Dirichlet-Neumann boundary conditions. Journal of Mathematical Analysis and Applications, 2024, 531(2): 127843.

[19] de Assis H R, Faria L F O. Elliptic equations involving supercritical sobolev growth with mixed dirichlet-neumann boundary conditions. Complex Variables and Elliptic Equations, 2024, 69(5): 713-728.

[20] Foss M, Radu P, Yu Y. Convergence analysis and numerical studies for linearly elastic peridynamics with dirichlet-type boundary conditions. Journal of Peridynamics and Nonlocal Modeling, 2023, 5(2): 275-310.